

CrystEngComm

Accepted Manuscript



This is an *Accepted Manuscript*, which has been through the Royal Society of Chemistry peer review process and has been accepted for publication.

Accepted Manuscripts are published online shortly after acceptance, before technical editing, formatting and proof reading. Using this free service, authors can make their results available to the community, in citable form, before we publish the edited article. We will replace this *Accepted Manuscript* with the edited and formatted *Advance Article* as soon as it is available.

You can find more information about *Accepted Manuscripts* in the [Information for Authors](#).

Please note that technical editing may introduce minor changes to the text and/or graphics, which may alter content. The journal's standard [Terms & Conditions](#) and the [Ethical guidelines](#) still apply. In no event shall the Royal Society of Chemistry be held responsible for any errors or omissions in this *Accepted Manuscript* or any consequences arising from the use of any information it contains.

1

2

The Culprit of Gout: Triggering Factors and

3

Formation of Monosodium Urate Monohydrate

4

5

Meng Hsiu Chih, Hung Lin Lee and Tu Lee*

6

Department of Chemical and Materials Engineering, National Central University,

7

300 Jhong-Da Road, Jhong-Li District, Taoyuan City 32001, Taiwan R.O.C.

8

9

10 ABSTRACT

11

Gout is a crystal-induced inflammatory arthritis by the deposition of

12

monosodium urate monohydrate (MSUM). Hyperuricemia is considered as an

13

essential factor for gout formation. However, *in vivo* MSUM crystallization

14

mechanism is still uncertain, and only some of the patients with hyperuricemia are

15

able to develop gout. Attempts were made to answer those unsolved questions based

16

on the experimental methods developed by Perrin and Swift including (1)

17

morphological studies of MSUM under various Na^+ ion levels, (2) pH effect and

18

conversion from uric acid dihydrate (UAD) to MSUM, and (3) synergistic effect of

*Corresponding Author. Telephone: +886-3-422-7151 ext. 34204. Fax: + 886-3-425-2296.

E-mail: tulee@cc.ncu.edu.tw

1 Na⁺, K⁺ and Ca²⁺ ions and hyaluronate chains on MSUM crystallization. Various
2 MSUM morphologies such as “beachball”, “urchin-like aggregate” and “bow-like
3 aggregate” could be prepared at different Na⁺ ion concentrations at 37°C.
4 Consequently, the pathogenesis of gout might be related to the MSUM morphological
5 transformation from “beachball” to needle. The conversion of UAD to MSUM was
6 studied by adjusting the pH value. The determined UAD-to-MSUM pathway was
7 thought to be followed by the MSUM deposition during phagocytosis when lactic
8 acid was present. In addition, a new type of MSUM “fishtail” morphology was
9 observed in the hyaluronate-, Na⁺ ions-, and Ca²⁺ ions-containing solutions. The
10 synergistic effect of hyaluronate and cations on the inhibition of MSUM
11 crystallization was further verified based on the crystal yields. The higher water
12 solubility of the hyaluronate-Ca-urate complex than the one of the urate ion might
13 explain why only a fraction of hyperuricemic patients developed gout. Although
14 there was no reported evidence about the complex, it was probable for it to minimize
15 the risk of gout formation in the hyperuricemic patients. Finally, the puzzle of gout
16 formation was pieced together and illustrated

17 **Keywords:** Gout, monosodium urate monohydrate (MSUM), hyaluronate, uric acid
18 dihydrate (UAD).

19

1 INTRODUCTION

2 Gout is a common inflammatory arthritis induced by the deposition of
3 monosodium urate monohydrate (MSUM) and might cause serious joint deformity
4 and disability. MSUM originated from uric acid ($pK_a = 5.75$), which is an
5 end-product of purine metabolism.^{1,2} Although MSUM had been identified over 100
6 years³ and its molecular structure and solid-state properties had also been well
7 characterized,⁴⁻¹¹ the prevalence and incidence of gout have continued to rise in the
8 US,¹² UK¹³ and Taiwan R.O.C.¹⁴ However, the *in vivo* crystallization mechanism
9 of MSUM is still uncertain to date.

10 MSUM crystal has a crystallographically triclinic structure.¹⁵ Its crystal
11 habit usually exhibits a needle shape, and rarely a spherical morphology for which the
12 two medical doctors, Fiechtner and Simkin, had dubbed the sphere “beachball”.^{7,8}
13 However, the “bow-like shaped” MSUM needle-clusters were often appeared *in vivo*
14 under the influence of biological substances.⁹ Besides, the MSUM clusters were
15 also reported to be produced in a buffer solution exceeding 100 mM of Na^+ ion.¹⁶
16 The many interesting morphological appearances of MSUM crystals have prompted
17 us to investigate the influence of Na^+ ions on MSUM crystal morphology.
18 Interestingly, the “beachball-like” MSUM morphology was seldom discussed and was
19 regarded as an amorphous form by others.⁶ For the biological strategy of making the

1 mineralized skeletons, a recent study suggested that stable crystals in living organisms
2 are usually developed by the transformation of the first-formed solids which are
3 usually disordered deposits.¹⁷ This crystallization strategy is widely discovered in
4 nature such as chiton teeth, mollusks shell and sea urchin spicules and spines.¹⁸
5 Therefore, we speculate that MSUM “beachballs” may serve as an essential transient
6 precursor during MSUM morphological evolution. Although the MSUM beachballs
7 had been prepared by quenching, the preparation method was completely deviated
8 from the *in vivo* conditions.^{6,7} Consequently, the first aim of our study is to
9 reproduce MSUM beachballs and its other morphologies under various Na⁺ ion levels
10 and to shed some light on the pathogenesis of gout.

11 Accordingly, there were several factors, which were considered to facilitate
12 the MSUM crystallization: (1) hyperuricemia,⁹ (2) temperature,¹⁹⁻²¹ (3) ionic
13 strength,^{4,19,21,22} (4) pH,²¹⁻²⁴ and (5) promoter/inhibitor molecules.^{22,25-27} Among
14 these factors, the temperature effect had been used to explain why MSUM is preferred
15 to crystallize out mainly in human joint and connective tissue. This is because the
16 lower local temperatures in joint and connective tissue than in other positions led to
17 the decrease in MSUM solubility. Some cations, biomolecules and proteins could
18 also affect the MSUM precipitation and be regarded as promoters or inhibitors. For
19 example, the presence of K⁺ ions would stabilize urate ions in an aqueous solution to

1 inhibit the crystallization of uric acid and MSUM.

2 The pH effect is related to inflammatory response²⁸ and acidosis.²⁹

3 Noticeably, the pH-solubility relationships of uric acid and MSUM in Figure S1

4 established by Wang and Königsberger²⁴ had shown that the solubility of MSUM

5 increases as the pH value decreases.^{22,24} However, this unusual observation is

6 against the fact that the decline in pH would promote the MSUM nucleation *in vitro*.²²

7 Moreover, uric acid is quite sensitive to pH fluctuation as reported in the renal

8 system.³⁰ There were three identified phases of uric acid, including uric acid

9 anhydrate (UAA), uric acid monohydrate (UAM), and uric acid dihydrate (UAD).

10 All of them were observed in the renal stone,³¹ and the relationships among UAA,

11 UAD and MSUM were shown in Scheme S1 of the Supplementary Information.

12 Therefore, the second aim of our study is to investigate the pH effect on MSUM

13 formation and the conversion from uric acid to MSUM in a simulated body fluid

14 (serum) system.

15 Hyperuricemia is an abnormally high level of uric acid in the blood when the

16 concentration of urate in serum is greater than 6.8 mg/dL. It is a prerequisite for the

17 MSUM deposition, but intriguingly, only a fraction of hyperuricemic subjects suffer

18 from gout disease.⁹ There seems to be physiological substances capable of

19 inhibiting urate crystallization. Individual synovial fluid component such as

1 hyaluronic acid had no significant effect on the growth rate constant of MSUM.²⁶
2 However, the interactions among hyaluronate chains, and Na⁺, K⁺ and Ca²⁺ ions³²
3 which are abundant in synovial fluid, may synergistically influence *in vivo* MSUM
4 crystallization. Therefore, the third aim is to explore the synergistic effect of
5 hyaluronate chains and various ions on MSUM crystallization.

6 **EXPERIMENTAL SECTION**

7 All chemicals were used as received without further purification and listed in
8 Table S1.

9 **Morphological studies of MSUM under various Na⁺ ion levels**

10 The method developed by Perrin and Swift¹¹ was modified and then used in
11 our studies. Solutions A and B were first prepared in a 37 °C water bath. 15 mL of
12 aqueous solution A was composed of (1) 13.3 mM of uric acid and (2) 15 mM of
13 NaOH. 5 mL of aqueous solution B was composed of (1) 20 mM of KCl, (2) 8 mM
14 of CaCl₂·2H₂O and (3) 400, 2400 or 6000 mM of NaCl, and the resulting solutions
15 were called B1, B2 and B3, respectively. The pH values of those solutions were
16 adjusted to 7.4 by 1 M HCl (aq) or 1 M NaOH (aq). Upon mixing of both solutions
17 A and B, the supersaturated solutions of MSUM containing of (1) 10 mM of uric acid,
18 (2) 5 mM of KCl, (3) 2 mM of CaCl₂·2H₂O and (4) 100, 600 or 1500 mM of NaCl,
19 respectively, were produced and were called C1, C2 and C3, respectively (Table 1).

1 Mixing the pre-dissolved solutions of A and B together was necessary to avoid the
2 occurrence of heterogeneous nucleation induced by undissolved NaCl, KCl and
3 $\text{CaCl}_2 \cdot 2\text{H}_2\text{O}$ solids. In a separate experiment, the concentration of NaCl was fixed to
4 1500 mM and MSUM crystals would be harvested after 2 months. All MSUM
5 crystals were filtered, rinsed by reversible osmosis water, oven dried at 40°C for 24 hr,
6 and characterized by polarized optical microscopy (POM), scanning electron
7 microscopy (SEM), Fourier-transform infrared spectroscopy (FT-IR), powder X-ray
8 diffraction (PXRD), and thermogravimetric analysis (TGA).

9 Based on the pH-solubility relationship shown in Figure S1, the saturation of
10 MSUM was around 0.26 mM in 150 mM Na^+ aqueous solution under the *in vivo*
11 normal condition of pH = 7.4 and 37°C as a reference.

12 **Effect of pH and conversion from UAD to MSUM**

13 Presores and Swift had discussed the conversion and transformation of uric
14 acid in urine-like systems³³ such as McIlvaine buffer and artificial urine solutions.³⁴
15 In this study, we chose the simulated body fluid (SBF)³⁵ to mimic synovial fluid
16 instead. SBF comprising 92.45 mM of NaCl, 8.81 mM of NaHCO_3 , 19.3 mM of
17 Na_2CO_3 , 3.02 mM of KCl, 1.01 mM of $\text{K}_2\text{HPO}_4 \cdot 3\text{H}_2\text{O}$, 1.50 mM of MgCl_2 , 0.5 mM
18 of Na_2SO_4 , and 50 mM of HEPES was prepared accordingly.³⁵ The pH value of
19 SBF was adjusted to 7.4 by 1 M NaOH (aq).

1 The very same procedure in the section of “Morphological studies of MSUM
2 under various Na⁺ ion levels” would be followed except for the Na⁺ ion concentration
3 which was fixed to 140 mM for simulating the *in vivo* condition.¹¹ Instead of using
4 1 M HCl (aq), about 10 mM aqueous solution of lactic acid³⁶ was chosen as an
5 acidosis factor²⁸ to lower the pH value to 5.0 to 5.8. Lowering the pH to an extreme
6 value of 5.0 was to accelerate the UAD formation within a reasonable time frame.
7 UAD solids were isolated after a few minutes, filtered, air dried for 10 min and stored
8 at -4 °C to prevent the dehydration of UAD to UAA.³⁷ About 30 mg of UAD solids
9 were dispersed in 3 mL of SBF at 37°C.³⁵ Solids were harvested for every 12-hr in a
10 total period of 36 hr, filtered, rinsed with RO water, air dried and characterized
11 immediately by POM and PXRD.

12 **Synergistic effect of Na⁺, K⁺ and Ca²⁺ ions, and hyaluronate chains on MSUM** 13 **crystallization**

14 Since the concentration of hyaluronate in normal joints ranges from 1.45 to
15 2.94 mg/mL,³⁸ 5 mL of aqueous solution D1 was composed of (1) 560 mM of NaCl
16 and (2) 40 mg of sodium hyaluronate. 5 mL of aqueous solution D2 was composed
17 of (1) 560 mM of NaCl, (2) 20 mM of KCl, and (3) 40 mg of sodium hyaluronate. 5
18 mL of aqueous solution D3 was composed of (1) 560 mM of NaCl, (2) 8 mM of
19 CaCl₂·2H₂O, and (3) 40 mg of sodium hyaluronate. 5 mL of aqueous solution D4

1 was composed of (1) 560 mM of NaCl, (2) 20 mM of KCl, (3) 8 mM of CaCl₂·2H₂O,
2 and (4) 40 mg of sodium hyaluronate. All aqueous solutions were prepared at 37°C
3 and their pH values were adjusted to 7.4 by 1M HCl (aq) or NaOH (aq). The
4 supersaturated solutions of MSUM, called E1, E2, E3 and E4, were prepared by
5 mixing solutions A and D1, D2, D3 and D4, respectively, and their compositions were
6 provided in Table 2. MSUM crystals would be harvested in 5 days, filtered, rinsed
7 by RO water, oven dried at 40°C for 24 hrs and characterized by POM and PXRD.

8 The constant composition method³⁹ developed by Nancollas et al. could
9 overcome the problems associated with the dynamically changing solution
10 composition during precipitation for many crystallization and mineralization kinetics
11 approaches. The concentrations of lattice ions were maintained constant by
12 simultaneous addition of reagent solutions and controlled by a glass electrode probe.
13 However, in our experiments, only the pH values of all the above-mentioned solutions
14 were checked to be around 7.4 by a pH meter due to its simplicity and robustness.

15 **RESULTS AND DISCUSSION**

16 **Morphological studies of MSUM under various Na⁺ ion levels**

17 POM images in Figure 1 showed that MSUM crystals grown under various
18 Na⁺ ion levels at 37°C were crystalline because of the strong birefringence. 200-300
19 μm radiating bow-like aggregates, 20-50 μm urchin-like aggregates, and 20-60 μm

1 “beachballs” were obtained under 100 mM, 600 mM, and 1500 mM Na⁺ ion levels,
2 respectively. It took two months for “beachballs” produced from 1500 mM solution
3 of Na⁺ ion to gradually evolve into “urchin-like” and “bow-like aggregates” (Figure
4 1d). The SEM images in Figure 2 showed that the “beachball” was composed of
5 many 1-2 μm-sized platelets filled with primary nanometer-sized needles.

6 All solids prepared at pH of 7.4 could guarantee that neither UAD nor UAA
7 was formed by FTIR spectra (Figure S2). All of MSUM crystals were verified
8 according to the characteristic IR peak assignments given in Table S2. The
9 relatively broad peaks with lower intensity in PXRD pattern (Figure S3) further
10 confirmed that “beachball” was composed of nanometer-sized crystallites with poor
11 crystallinity based on Scherrer’s formula.^{40,41} In TGA scans (Figure S4), the first
12 weight losses for both of “bow-like aggregates” and “beachball” were about 7.2 %
13 approximating to the weight percent of hydrate within the crystal lattice of MSUM.
14 However, the dehydration temperature for “beachball” was around 100°C, which was
15 lower than the one for “bow-like” at 150°C. It might be attributed to the relatively
16 large surface area of MSUM beachball for accelerating the dehydration process.
17 They began to degrade when heated to over 300°C.

18 Our *in vitro* experiments suggested that “beachball”, “urchin-like aggregate”
19 and “bow-like aggregate” were related to the Na⁺ ion levels (Figure 1) and not just

1 only to the biological⁹ and/or macromolecular⁴² components in synovial fluid as
2 claimed by others.^{9,42} All MSUM morphologies were mutually related to one
3 another because the first-formed metastable “beachballs” could transform to
4 “urchin-like aggregate” and then to “bow-like shaped” clusters or needle-shaped
5 crystals in solution if given long enough time. According to SEM images in Figure
6 2, we proposed that MSUM “beachball” might be a mesocrystal having a hierarchical
7 structure⁴³ via an aggregation-mediated pathway by nano-clusters instead of merely
8 amplification in crystal growth.⁴⁴ However, more studies for the exact pathway
9 would still be needed in the future.

10 Since “beachballs” were only discovered in a hypertensive female patient who
11 also required weekly peritoneal dialysis,⁸ it was speculated that the local fluctuation
12 of Na⁺ ion level or other conditions raising MSUM supersaturation level in her
13 synovial fluid might play a dominant role in “beachball” formation. The
14 pathogenesis of gout may be related to the MSUM morphological transformation
15 from “beachball” to needle.⁸

16 **Effect of pH and conversion from UAD to MSUM**

17 Within a few minutes upon the addition of lactic acid, the pH was first reduced
18 to 5.0 and then increased to 5.8 gradually as UAD plates were being precipitated out.
19 Lowering the pH value to 5.0 was to accelerate the UAD crystallization, and UAD

1 crystals would precipitate after the pH value was lowered to 5.5. UAD plates were
2 then isolated and converted in a freshly prepared SBF environment to induce the
3 transformation from UAD to MSUM. The POM images and PXRD patterns for
4 UAA, UAD and MSUM also were provided in Figure S5 for comparison. Based on
5 the crystal habits, the POM images in Figure 3 showed that the integrity of UAD
6 plates was partially maintained during dissolution in the first 12 hr. The UAD plates
7 were bristled and covered with many tiny crystals 24 hr later. UAD plates were
8 disappeared after 36 hr and needle-shaped MSUM crystals were found 48 hr later.

9 PXRD patterns in Figure 4 illustrated the conversion of UAD to MSUM
10 thoroughly. Intense diffraction lines for UAD³³ were at $2\theta = 10^\circ$ and 20° , for UAA³³
11 was at $2\theta = 13.5^\circ$, and for MSUM⁴⁶ were at $2\theta = 11.6^\circ$, 18.9° and 28.3° . The
12 PXRD patterns in Figures 3(d) and 4(d) also revealed that UAD took 36 hr to convert
13 to MSUM, and UAA was an intermediate phase coexisting with UAD in 24 hr (Figure
14 4(c)). Finally, MSUM needles would be grown completely after 48 hr later (Figures
15 3(e) and 4(e)). TGA scans of UAD and UAA were shown in Figure S6.

16 Under the normal physiological Na^+ ion concentration of approximately 140
17 mM,²² the dominant MSUM morphology was “bow-like aggregates” (Figure 1) which
18 were strikingly similar to the native crystals formed in cartilage.⁹ As for the gout
19 formation mechanism in humans, a fundamental question still remains: How does the

1 MSUM crystal appear initially? Most likely, the triggering factor is the local pH
2 reduction in connective tissues and joints²⁵ brought about by the inflammatory
3 reaction²⁸ and acidosis.²⁹ The sudden decline of local pH did favor the rapid
4 formation of UAD plates more than MSUM crystals according to their solubility
5 behaviors.^{24,37} However, as the pH was returned to about 7.4,⁴⁷ the conversion from
6 UAD to MSUM would be activated and finished after 36 hr (Figure 4). Therefore,
7 UAD crystals are likely to be the triggering factor for *in vivo* gout formation.

8 This UAD-to-MSUM conversion could offer a more reasonable time frame in
9 human life for gout deposition by acidosis than the time required for direct MSUM
10 crystallization. The growth rate of MSUM crystal at its favorable pH²³ of 7.0 and a
11 urate concentration of 0.6 mM (i.e. > 6.8 mg/dL, hyperuricemia)¹ was calculated to be
12 only 10⁻¹¹ μm/min.⁴⁸ However, UAD crystals could precipitate immediately with the
13 temporary decline of local pH value, and UAD would then convert to MSUM at a
14 normal pH value (pH = 7.4) during a relatively short time. The UAD-to-MSUM
15 pathway offered an explanation to the appearance of MSUM crystals in cartilage,
16 synovial and tendon sheaths²⁵ because of the pH gradient between human plasma and
17 tissue.²⁸ Furthermore, acute gouty arthritis would develop when MSUM needles
18 were ingested by leucocytes. During phagocytosis, the production of lactic acid
19 would further provoke MSUM deposition according to the UAD-to-MSUM pathway.

1 This self-sustaining cycle provided a stimulus to a greater inflammatory response.²⁸

2 **Synergistic effect of Na⁺, K⁺ and Ca²⁺ ions, and hyaluronate chains on MSUM**

3 **crystallization**

4 Solids grown in aqueous solutions with sodium hyaluronate and various
5 cations were identified to be MSUM by PXRD (Figure S7) and the crystal yield for
6 each condition was weighted. Because hyaluronate chain would interact with Na⁺,
7 K⁺ and Ca²⁺ ions,³² we broke down the study of those interactions among hyaluronate
8 and cations into four parts. POM images in Figure 5 showed that the number of
9 MSUM crystals decreased as more types of cations were added into the
10 hyaluronate-containing solutions. A new type of MSUM “fishtail” morphology was
11 observed in the hyaluronate-, Na⁺ ions-, and Ca²⁺ ions-containing solutions (Figure 5).
12 The synergistic effect of hyaluronate and cations on the inhibition of MSUM
13 crystallization was further verified based on the crystal yields (Table S3). SBF with
14 the coexistence of physiological concentrations of hyaluronate, Na⁺, K⁺ and Ca²⁺ ions
15 gave the minimum MSUM crystal yield of 7.2 wt % which was at least six times less
16 than the crystal yield of 47.3 % from the SBF having only hyaluronate and Na⁺ ions.
17 The saturation values of MSUM in solutions of E1 to E4 were determined and
18 summarized in Table S3.

19 Moreover, Ca²⁺ ion was normally believed to reduce the solubility of MSUM,

1 and the initial nucleus for gout was thought to be calcium urate.^{22,49} However, our
2 findings of the synergistic effect of hyaluronate chains and Ca^{2+} ions and even with
3 Na^+ and K^+ ions have shown the otherwise.³² The dominant role of Ca^{2+} ions might
4 have been a crystal inhibitor for MSUM deposition instead (Table S3). Since
5 hyaluronate chains contain hydrophilic hydroxyl ($-\text{OH}$) and carboxylate ($-\text{COO}^-$)
6 pendent groups, hyaluronate chains are water soluble. With the presence of Ca^{2+}
7 ions and other cations acting as salt bridges between the $-\text{COOH}^-$ groups of
8 hyaluronate chains and the N3 ($\text{pK}_a = 5.75$) sites^{1,50} on the six-member ring of the
9 urate ion, the slightly soluble urate ion has now become a solubilized complex in
10 water thanks to the high solubility power of hyaluronate. The higher water solubility
11 of the hyaluronate-Ca-urate complex than the one of the urate ion might be one of the
12 reasons for only a fraction of hyperuricemic patients to develop gout. Although
13 there was no reported evidence about the complex, it was probable for it to minimize
14 the risk of gout formation in the hyperuricemic patients. If the complex was
15 disrupted, MSUM deposition would occur.

16 Furthermore, the interactions among hyaluronate chains, Na^+ and Ca^{2+} ions
17 produced fishtail MSUM clusters (Figure 5). Interestingly, the fishtail clusters had
18 never been reported in gouty patients. Fishtail clusters should have appeared if
19 hyaluronate, Na^+ ion and Ca^{2+} ion were all abundant in gouty patient's synovial fluid.

1 This implied that the decrease in production, polymerization, molecular size and
2 concentration of hyaluronate chains during inflammation³⁸ had prevented the
3 formation of hyaluronate-Ca-urate complex, and thus, only the usual bow-like MSUM
4 aggregates were grown.

5 Finally, our hypothesis of gout formation was illustrated in Figure 6. Local
6 pH decline and the disruption of hyaluronate-Ca²⁺-urate complex are the triggering
7 factors for gout formation. Local pH decline could induce UAD crystals formation
8 at first, and UAD would convert to MSUM after the return of the pH value. The
9 dissolution of UAD may promote MSUM crystallization due to the increase of local
10 urate level. The rise of the concentration Na⁺ ions (or the increase of the urate ions
11 level) could increase the degree of supersaturation, and this driving force may
12 promote the “beachball” formation. In addition, MSUM crystals would induce acute
13 gouty arthritis due to leucocytes, and this could decrease the local pH again. This
14 self-sustaining vicious cycle provided a stimulus to an even greater inflammatory
15 response.

16 CONCLUSIONS

17 Seven key lessons were learned in this study: (1) Various morphologies of
18 MSUM: “beachball”, urchin-like and bow-like aggregates could be prepared under
19 different Na⁺ ion levels at 37°C. (2) Morphological transformation from “beachball”

1 to urchin-like aggregate to bow-like aggregate can be achieved. (3) “Beachball” is a
2 metastable first-formed precursor for all MSUM morphologies. (4) A new type of
3 MSUM fishtail morphology was observed in the hyaluronate, Na^+ , Ca^{2+} ion
4 containing solutions. (5) The dilemma of MSUM deposition at thermodynamically
5 unfavorable low pH condition was plausibly solved by the kinetic pathway for the
6 phase transformation of UAD to MSUM in the gout study. (6) The UAD-to-MSUM
7 pathway can also be used to explain the effects brought about by the inflammatory
8 response and acidosis, and why MSUM deposition in cartilage and connective tissue.
9 (7) The question of why only a fraction of hyperuricemic patients has gout might be
10 answered by the solubilization of urate through complex formation with hyaluronate
11 chains and Ca^{2+} ions.

12

13 ACKNOWLEDGMENTS

14 This research was supported by the grants from the Ministry of Science and
15 Technology of Taiwan, R.O.C. (MOST 102-2221-E-008 -071-MY2 &
16 104-2221-E-008-070-MY3). We are greatly indebted to Ms. Ching-Tien Lin for the
17 assistance with SEM, Ms. Shew-Jen Weng for PXRD, and all with the Precision
18 Instrument Center at National Central University.

FIGURE LEGENDS

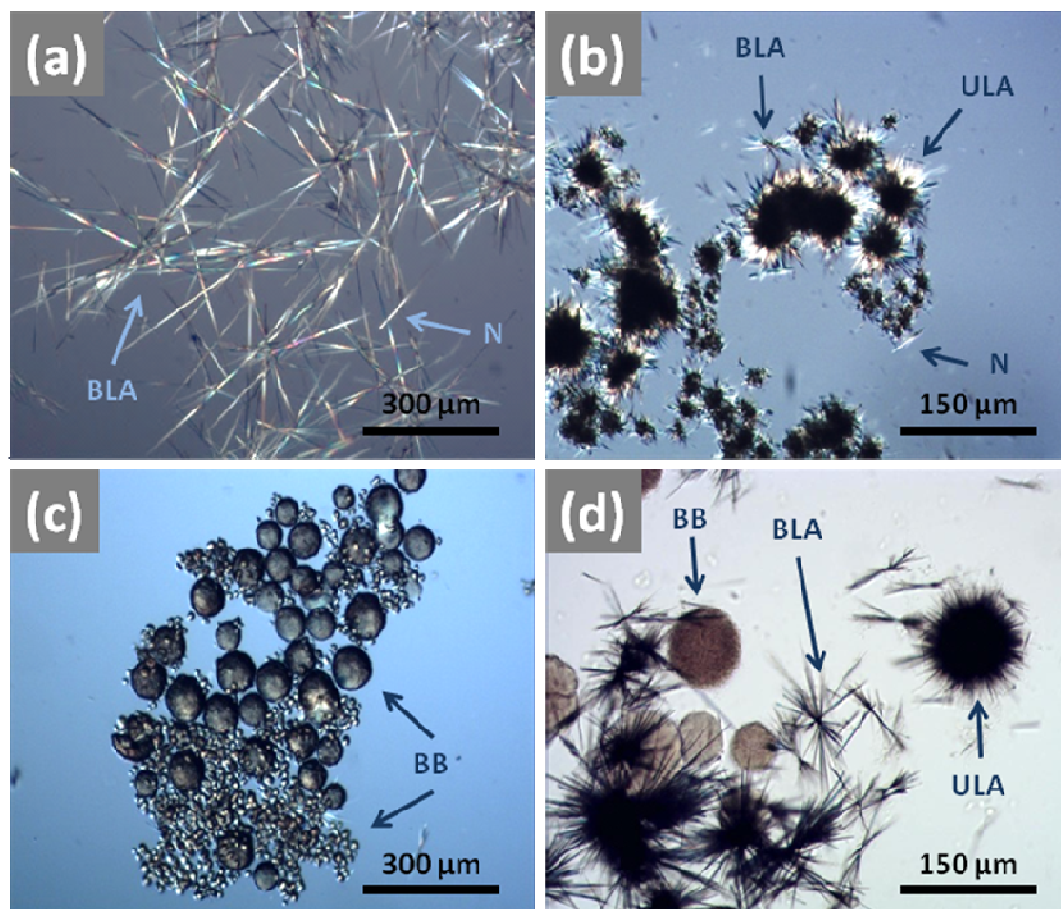


Figure 1. POM images of MSUM grown: (a) in 100 mM Na^+ ion for 2 days, (b) in 600 mM Na^+ ion for 2 days, (c) in 1500 mM Na^+ ion for 2 days, and (d) in 1500 mM Na^+ ion after 2 months (N: needle; BLA: bow-like aggregate; ULA: urchin-like aggregate; BB: beachball).

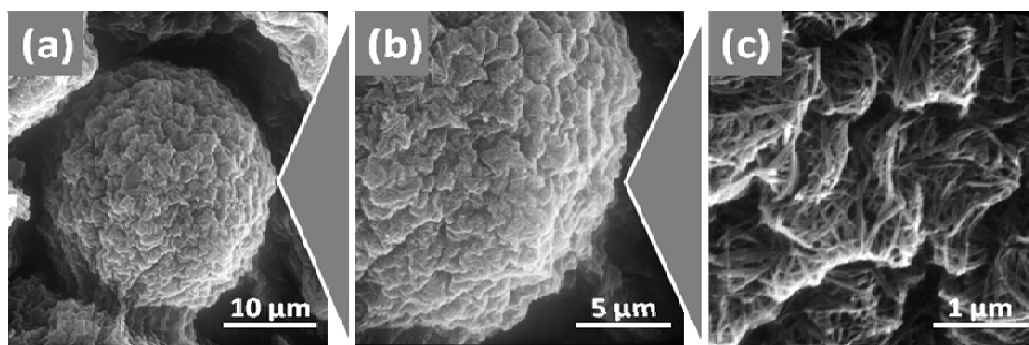


Figure 2. SEM images of a MSUM beachball grown in 1400 mM Na⁺ ion for 2 days at various magnifications: (a) a full view of “beachball”, (b) oriented platelets, and (c) primary nanometer-sized needles.

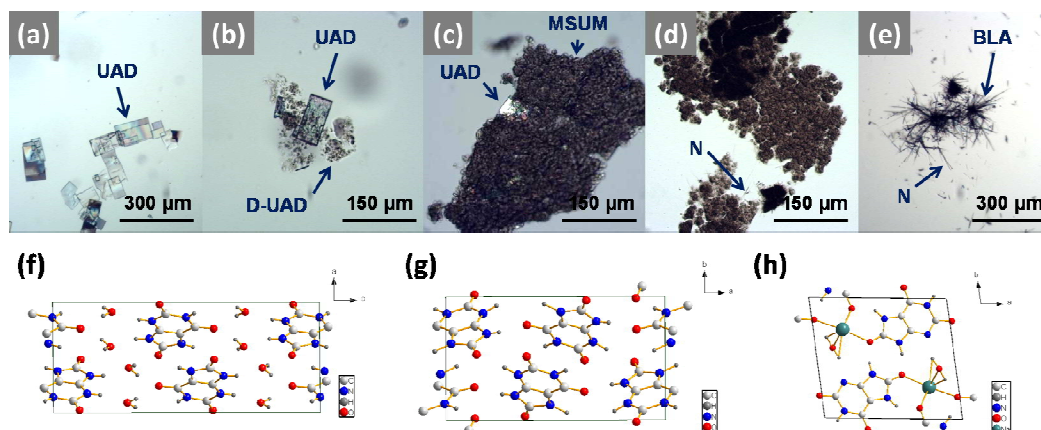


Figure 3. POM images during the conversion of UAD to MSUM: (a) initial UAD plates, (b) UAD plates with partially dissolved fragments at 12 hr (D-UAD: dissolved UAD fragments), (c) UAD plates covered with MSUM tiny crystals at 24 hr, (d) aggregation of MSUM tiny needles at 36 hr, (e) well-grown MSUM needles at 48 hr (N: needle; BLA: bow-like aggregate), (f) view of crystal structure of UAD showing the top view along the b-axis, constructed from fractional coordinates in refcode: ZZZPPI02,^{45a} (g) view of crystal structure of UAA showing the top view along the c-axis, constructed from fractional coordinates in refcode: URICAC,^{45b} and (h) view of crystal structure of MSUM showing the top view along the c-axis, constructed from fractional coordinates in refcode: NAURAT.¹⁵

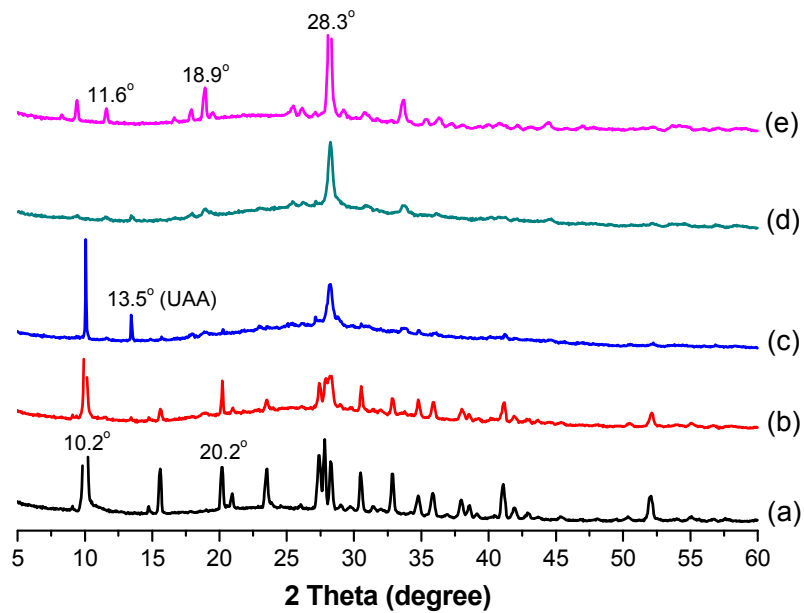


Figure 4. PXRD patterns of solids harvested from SBF during the conversion of UAD to MSUM at (a) 0 hr (UAD), (b) 12 hr (UAD), (c) 24 hr (UAD and UAA), (d) 36 hr (MSUM), and (e) 48 hr (MSUM).

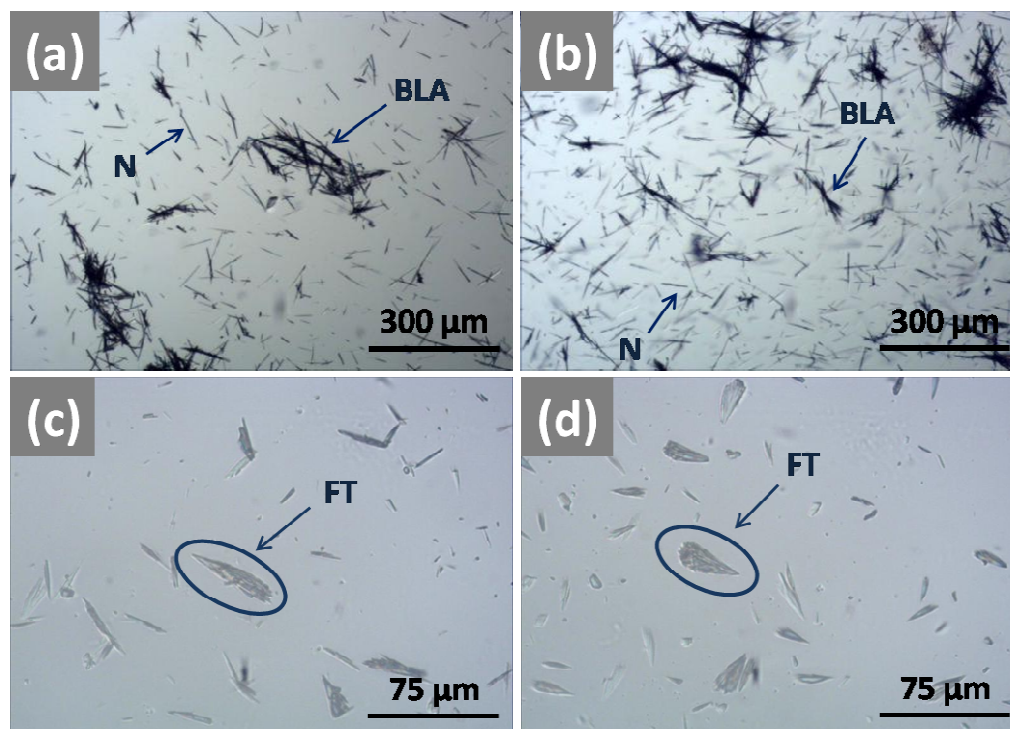


Figure 5. POM images of MSUM crystals grown in solutions: (a) E1: 2 mg/mL of sodium hyaluronate and 140 mM of Na^+ ion, (b) E2: 2 mg/mL of sodium hyaluronate, 140 mM of Na^+ ion and 5 mM of K^+ ion, (c) E3: 2 mg/mL of sodium hyaluronate, 140 mM of Na^+ ion and 2 mM of Ca^{2+} ion, (d) E4: 2 mg/mL of sodium hyaluronate, 140 mM of Na^+ ion, 5 mM of K^+ ion and 2 mM of Ca^{2+} ion (N: needle; BLA: bow-like aggregate; FT: fishtail).

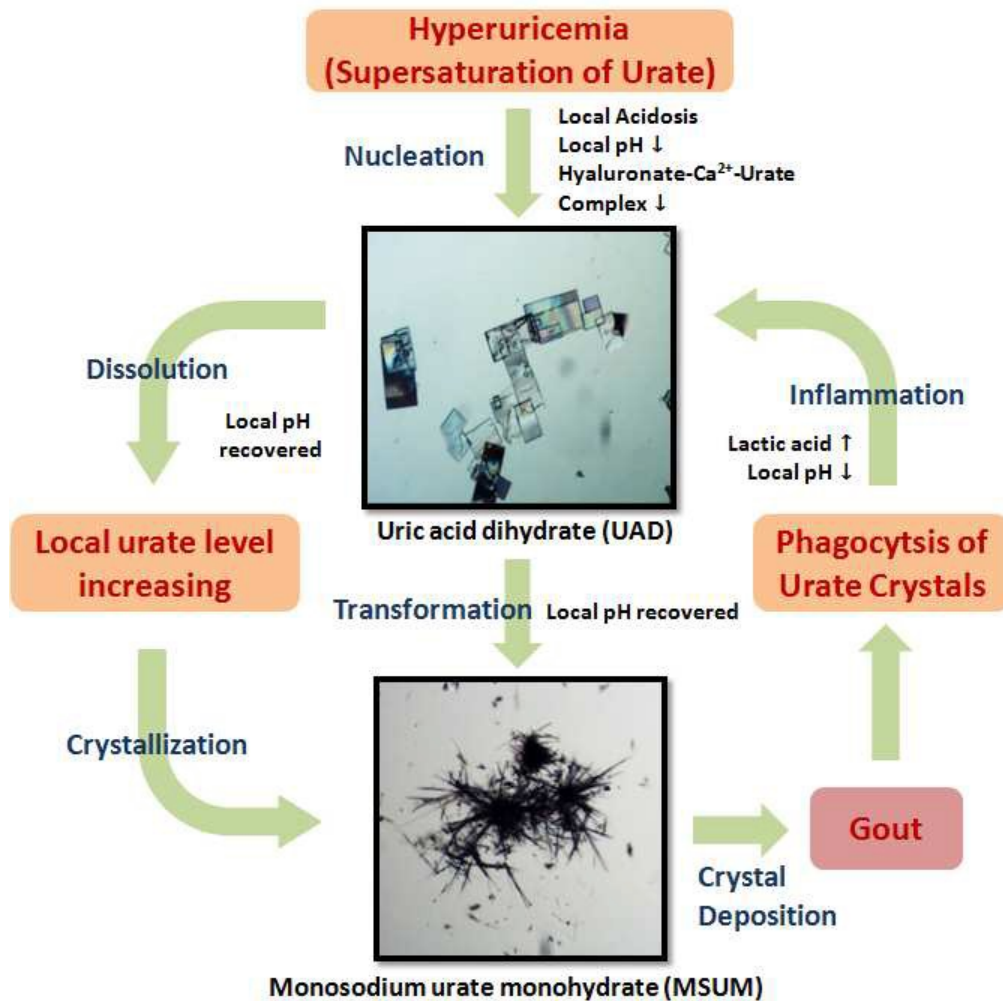


Figure 6. Triggering factors, proposed mechanism and self-sustaining cycle for the crystallization of MSUM and gout.

TABLE LEGENDS

Table 1. The compositions and conditions of supersaturated MSUM solutions under the various Na⁺ ion levels for MSUM morphological studies.

Composition/Condition	Solution C1	Solution C2	Solution C3
Uric acid	10 mM	10 mM	10 mM
NaCl	100 mM	600 mM	1500 mM
KCl	5 mM	5 mM	5 mM
CaCl₂·2H₂O	2.5 mM	2.5 mM	2.5 mM
pH	7.4	7.4	7.4
Temperature	37°C	37°C	37°C

Table 2. The compositions and conditions of supersaturated MSUM solutions for synergistic effect of Ca^{2+} , K^+ and Na^+ ions and hyaluronate chains on MSUM crystallization.

Composition/Condition	Solution E1	Solution E2	Solution E3	Solution E4
Uric acid	10 mM	10 mM	10 mM	10 mM
NaCl	140 mM	140 mM	140 mM	140 mM
KCl	-	5 mM	-	5 mM
$\text{CaCl}_2 \cdot 2\text{H}_2\text{O}$	-	-	2.5 mM	2.5 mM
Sodium Hyaluronate	2 mg/mL	2 mg/mL	2 mg/mL	2 mg/mL
pH	7.4	7.4	7.4	7.4
Temperature	37°C	37°C	37°C	37°C

REFERENCES

- ¹ F. Oliviero, A. Scanu, L. Punzi., *Reumatismo*, 2011, **63**, 221-229.
- ² A. Chhana, N. Dalbeth, *Rheum. Dis. Clin. North Am.*, 2014, **40**, 291-309.
- ³ W. A. Katz, *Arthritis Rheum.*, 1975, **18**, 751-756.
- ⁴ H.-K. Tak, W. R. Wilcox, S. M. Cooper, *J. Colloid Interface Sci.*, 1980, **77**, 195-201.
- ⁵ N. S. Mandel, *Arthritis Rheum.*, 1980, **23**, 772-776.
- ⁶ J. E. Seegmiller, R. R. Howell, S. E. Malawista, *JAMA-J. Am. Med. Assoc.*, 1962, **180**, 469-475.
- ⁷ J. J. Fiechtner, P. A. Simkin, *Adv. Exp. Med. Biol.*, 1980, **122A**, 141-143.
- ⁸ J. J. Fiechtner, P. A. Simkin, *JAMA-J. Am. Med. Assoc.*, 1981, **245**, 1533-1536.
- ⁹ N. W. McGill, A. Hayes, P. A. Dieppe, *Scand. J. Rheumatol.*, 1992, **21**, 215-219.
- ¹⁰ H. Paul, A. J. Reginato, H. R. Schumacher, *Ann. Rheum. Dis.*, 1983, **42**, 75-81.
- ¹¹ C. M. Perrin, J. A. Swift, *CrystEngComm*, 2012, **14**, 1709-1715.
- ¹² Y. Zhu, B. J. Pandya, H. K. Choi, *Arthritis Rheum.*, 2011, **63**, 3136-3141.
- ¹³ C.-F. Kuo, M. J. Grainge, C. Mallen, W. Zhang, M. Doherty, *Ann. Rheum. Dis.*, 2014, **74**, 661-667.
- ¹⁴ C.-F. Kuo, K.-H. Yu, L.-C. See, I.-J. Chou, Y.-S. Ko, H.-C. Chang, M.-J. Chiou, S.-F. Luo, *Rheumatology*, 2013, **52**, 111-117.

-
- ¹⁵ N. S. Mandel, G. S. Mandel, *J. Am. Chem. Soc.*, 1976, **98**, 2319-2323.
- ¹⁶ H.-K. Tak, S. M. Cooper, W. R. Wilcox, *Arthritis Rheum.*, 1980, **23**, 574-580.
- ¹⁷ S. Weiner, I. Sagi, L. Addadi, *Science*, 2005, **309**, 1027-1028.
- ¹⁸ A.-W. Xu, Y. Ma, H. Cölfen, *J. Mater. Chem.*, 2007, **17**, 415-449.
- ¹⁹ D. J. Allen, G. Milosovich, A. M. Mattocks, *Arthritis Rheum.*, 1965, **8**, 1123-1133.
- ²⁰ J. N. Loeb, *Arthritis Rheum.*, 1972, **15**, 189-192.
- ²¹ I. Kippen, J. R. Klinenberg, A. Weinberger, W. R. Wilcox, *Ann. Rheum. Dis.*, 1974, **33**, 313-317.
- ²² W. R. Wilcox, A. A. Khalaf, *Ann. Rheum. Dis.*, 1975, **34**, 332-339.
- ²³ W. R. Wilcox, A. Khalaf, A. Weinberger, I. Kippen, J. R. Klinenberg, *Med. Biol. Eng.*, 1972, **10**, 522-531.
- ²⁴ Z. Wang, E. Königsberger, *Thermochim. Acta*, 1998, **310**, 237-242.
- ²⁵ W. A. Katz, M. Schubert, *J. Clin. Invest.*, 1970, **49**, 1783-1789.
- ²⁶ H. M. Burt, Y. C. Dutt, *Ann. Rheum. Dis.*, 1986, **45**, 858-864.
- ²⁷ H. M. Burt, Y. C. Dutt, *J. Cryst. Growth*, 1989, **94**, 15-22.
- ²⁸ J. E. Seegmiller, R. Rodney Howell, *Arthritis Rheum.*, 1962, **5**, 616-623.
- ²⁹ M. A. Martillo, L. Nazzal, D. B. Crittenden, *Curr. Rheumatol. Rep.*, 2014, **16**, 400.
- ³⁰ H. Iwata, S. Nishio, M. Yokoyama, A. Matsumoto, M. Takeuchi, *J. Urol.*, 1989, **142**, 1095-1098.

-
- ³¹ G. Schubert, G. Reck, H. Jancke, W. Kraus, C. Patzelt, *Urol. Res.*, 2005, **33**, 231-238.
- ³² J. K. Sheehan, C. Arundel, C. F. Phelps, *Int. J. Biol. Macromol.*, 1983, **5**, 222-228.
- ³³ J. B. Presores, J. A. Swift, *CrystEngComm*, 2014, **16**, 7278-7284.
- ³⁴ T. C. McIlvaine, *J. Biol. Chem.*, 1921, **49**, 183-186.
- ³⁵ A. Oyane, H.-M. Kim, T. Furuya, T. Kokubo, T. Miyazaki, T. Nakamura, *J. Biomed. Res. A.*, 2003, **65**, 188-195.
- ³⁶ K. Kaneko, M. Maru, *Anal. Biochem.*, 2000, **281**, 9-14.
- ³⁷ F. Grases, A. I. Villacampa, A. Costa-Bauzá, O. Söhnle, *Scanning Microsc.*, 1999, **13**, 223-234.
- ³⁸ R. K. Strachan, P. Smith, D. L. Gardner, *Ann. Rheum. Dis.*, 1990, **49**, 949-952.
- ³⁹ (a) M. B. Tomson, G. H. Nancollas, *Science*, 1978, **200**, 1059-1060. (b) P. Koutsoukos, Z. Amjad, M. B. Tomson, G. H. Nancollas, *J. Am. Chem. Soc.*, 1980, **102**, 1553-1557. (c) T. J. Halter, B. M. Borah, B. Xie, G. H. Nancollas, *Colloid Surf. A Physicochem. Eng. Asp.*, 2015, **482**, 300-305.
- ⁴⁰ H. P. Klug, L. E. Alexander, *Crystallite size and lattice strains from line broadening*, Wiley, New York, 2nd ed., 1974, Chapter 9, pp 657-661.
- ⁴¹ F. Qian, J. Tao, S. Desikan, M. Hussain, R. L. Smith, *Pharm. Res.*, 2007, **24**, 1551-1560.

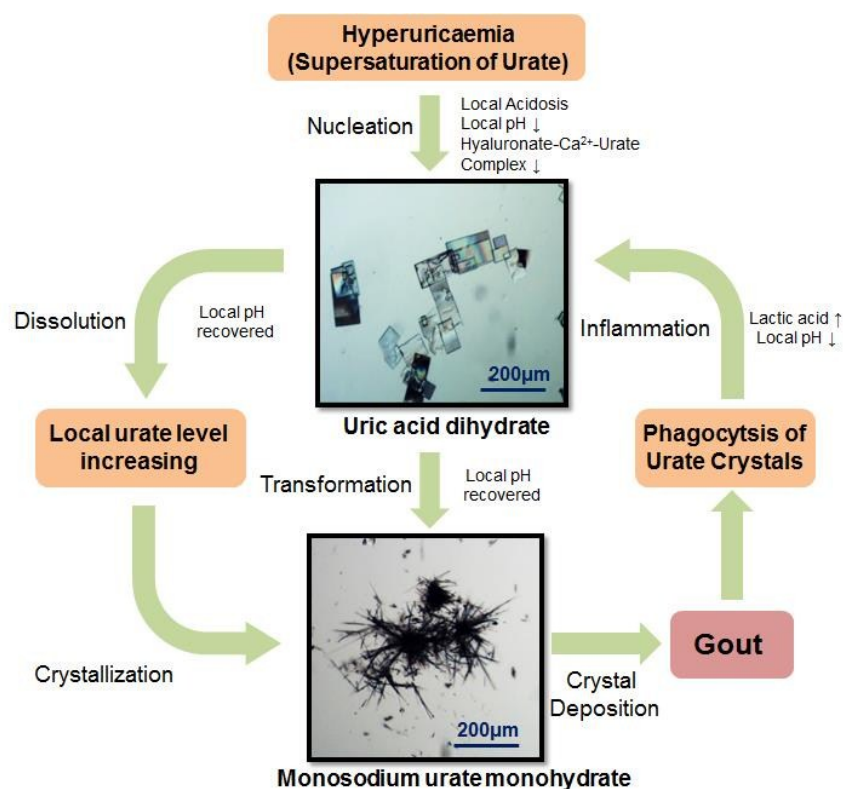
-
- ⁴² S. N. Kalkura, E. K. Girija, M. Kanakavel, P. Ramasamy, *J. Mater. Sci.-Mater. Med.*, 1995, **6**, 577-580.
- ⁴³ A.-W. Xu, M. Antonietti, H. Cölfen, Y.-P. Fang, *Adv. Funct. Mater.*, 2006, **16**, 903-908.
- ⁴⁴ (a) M. Niederberger, H. Cölfen, *Phys. Chem. Chem. Phys.*, 2006, **8**, 3271-3287. (b) T. Lee, C. W. Zhang, *Pharm. Res.*, 2008, **25**, 1563-1571.
- ⁴⁵ (a) H. Ringertz, *Acta Crystallogr.*, 1966, **20**, 397-403. (b) S. Parkin, H. Hope, *Acta Crystallogr. B*, 1998, **B54**, 339-344.
- ⁴⁶ B. B. Parekh, S. R. Vasant, K. P. Tank, A. Raut, A. D. B. Vaidya, M. J. Joshi, *Am. J. Infect. Dis.*, 2009, **5**, 225-230.
- ⁴⁷ P. S. Treuhaft, D. J. McCarty, *Arthritis Rheum.*, 1971, **14**, 475-484.
- ⁴⁸ P. D. Calvert, R. W. Fiddis, N. Vlachos, *Colloid Surf.*, 1985, **14**, 97-107.
- ⁴⁹ A. A. Khalaf, W. R. Wilcox, *J. Cryst. Growth*, 1973, **20**, 227-232.
- ⁵⁰ S. Satter, M. J. Carroll, A. A. Sargeant, J. A. Swift, *CrystEngComm*, 2008, **10**, 155-157.

Graphics of Contents:

The Culprit of Gout: Triggering Factors and Formation of Monosodium Urate Monohydrate

M. H. Chih and T. Lee*

Department of Chemical & Materials Engineering, National Central University,
300 Jhongda Road, Jhongli District, Taoyuan City 32001, Taiwan R.O.C.



Triggering factors, proposed mechanism and self-sustaining cycle for the crystallization of MSUM and gout.

* Corresponding author: tulee@cc.ncu.edu.tw

